# Natural killer cell recruitment and activation are regulated by CD47 expression in the tumor microenvironment

**Pulak Ranjan Nath**[1,*,§], **Dipasmita Pal-Nath**[1], **Ajeet Mandal**[2], **Margaret C. Cam**[3], **Anthony L. Schwartz**[1], **David D. Roberts**[1,*]

[1]Laboratory of Pathology, Center for Cancer Research, National Cancer Institute, National Institutes of Health, Bethesda, MD, USA

[2]Human Brain Collection Core, National Institute of Mental Health, National Institutes of Health, Bethesda, MD, USA

[3]CCR Collaborative Bioinformatics Resource, Office of Science and Technology Resources, National Cancer Institute and Leidos Biomedical Research, Inc., National Institutes of Health, Bethesda, MD, USA

## Abstract

Elevated CD47 expression in some cancers is associated with decreased survival and limited clearance by phagocytes expressing the CD47 counter-receptor SIRPα. In contrast, elevated CD47 mRNA expression in human melanomas was associated with improved survival. Gene expression data was analyzed to determine a potential mechanism for this apparent protective function and suggested that high CD47 expression increases recruitment of natural killer (NK) cells into the tumor microenvironment. The CD47 ligand thrombospondin-1 inhibited NK cell proliferation and CD69 expression *in vitro*. *Cd47*$^{-/-}$ NK cells correspondingly displayed augmented effector phenotypes, indicating an inhibitory function of CD47 on NK cells. Treating human NK cells with a CD47 antibody that blocks thrombospondin-1 binding abrogated its inhibitory effect on NK cell proliferation. Similarly, treating wildtype mice with a CD47 antibody that blocks thrombospondin-1 binding delayed B16 melanoma growth, associating with increased NK cell recruitment and increased granzyme B and interferon-$\gamma$ levels in intratumoral NK but not CD8$^+$ T cells. However, B16 melanomas grew faster in *Cd47*$^{-/-}$ versus wildtype mice. Melanoma-bearing *Cd47*$^{-/-}$ mice exhibited decreased splenic NK cell numbers with impaired effector protein expression and elevated exhaustion markers. Pro-apoptotic gene expression in *Cd47*$^{-/-}$ NK cells was associated with stress-mediated increases in mitochondrial proton leak, reactive oxygen species, and apoptosis. Global gene expression profiling in NK cells from tumor-bearing mice identified CD47-dependent transcriptional responses that regulate systemic NK activation and exhaustion. Therefore, CD47 positively and negatively regulates NK cell function, and therapeutic

*Correspondence: Dr. David D. Roberts, droberts@mail.nih.gov, Dr. Pulak R. Nath, hellopran2000@gmail.com.
§Current address: The Jackson Laboratory for Genomic Medicine, Farmington, CT, USA

potential conflicts of interest are disclosed online

antibodies that block inhibitory CD47 signaling can enhance NK immune surveillance of melanomas.

## Introduction

CD47 is a transmembrane protein that interacts with several integrins, two signal-regulatory protein (SIRP) family counter-receptors, and the secreted protein thrombospondin-1 (1–3). Malignant cells in some hematopoietic malignancies and solid tumors express elevated levels of CD47 relative to healthy tissues, and elevated CD47 in some cancers is correlated with poor prognosis (4). The prevailing hypothesis is that interaction of tumor cell CD47 with the counter-receptor SIRPα on macrophages inhibits phagocytosis of tumor cells (4). Conversely, antibody-mediated blockade of SIRPα binding or knockdown of CD47 promotes active phagocytosis of implanted human xenograft tumors in mice expressing a variant of SIRPα that binds human CD47 with high affinity (4,5). In contrast, blocking SIRPα binding to CD47 is generally not sufficient to promote phagocytic clearance of syngeneic tumors in immune-competent mice, which requires additional immune stimuli to induce CD8 T cell-mediated tumor killing (4,6,7). CD47 is an inhibitory signaling receptor for thrombospondin-1 on T cells (8,9). Thrombospondin-1 signaling through CD47 also inhibits antigen presentation by dendritic cells to T cells (10). CD47 is, therefore, an innate and adaptive immune checkpoint.

We found that natural killer (NK) cells express high levels of CD47 mRNA and cell surface protein, which regulates NK cell homeostasis and their response to viral infection in mice (11). NK cells are also a first line of defense system against malignant cell transformation (12–14).

NK cell development, education and effector functions are regulated by several families of activating and inhibitory receptors, including the killer cell immunoglobulin-like receptor (KIR) family, the CD94 family and the leukocyte immunoglobulin-like receptor (LIR) family, NKG2D and the natural cytotoxicity receptors (NCRs) NKp30, NKp44 and NKp46 (15). Inhibitory NK receptors recognize MHC class I, as well as non-MHC-I ligands such as PVR (15–19). The regulatory roles of thrombospondin-1 and CD47 in NK cells are less clear. Thrombospondin-1 inhibits early NK cell proliferation and enhances late expansion, but a role for CD47 in these activities was not examined (20). Functioning as a SIRPα counter-receptor, CD47 enables engraftment of NK precursors in mice reconstituted with a human immune system (21). Treatment with a CD47 antibody that inhibits SIRPα and thrombospondin-1 binding increased NK cell killing of head-and-neck squamous carcinoma cells *in vitro*, but the mechanism remains unclear because NK cells are not known to express SIRPα (22). Depletion of NK cells similarly attenuated the anti-tumor activity of a SIRPα blocking antibody in a syngeneic murine renal carcinoma model, but the same antibody did not inhibit NK killing of the tumor cells *in vitro*, suggesting a SIRPα-independent function of CD47 in NK cells (23).

Analysis of The Cancer Genome Atlas (TCGA) data for human melanomas, showed positive correlations between CD47 mRNA expression and patient survival and CD47 expression with the expression of NK early activation genes. We identified CD47-dependent inhibitory

functions for thrombospondin-1 in human and murine NK cells *in vitro*. Correspondingly, inhibition of melanoma growth following treatment with a CD47 antibody that inhibits thrombospondin-1 binding was associated with enhanced NK cell activation. In contrast, B16 melanoma tumors grew faster in $Cd47^{-/-}$ mice, which was associated with reduced NK frequency and enhanced NK exhaustion, similar to that observed during chronic LCMV infection of $Cd47^{-/-}$ mice (11). Gene expression and functional studies in NK cells identified impaired mitochondrial function and an enhanced proapoptotic signature in $Cd47^{-/-}$ NK cells when subjected to stress. Therefore, we demonstrated that CD47 has both positive and negative roles in regulating antitumor NK immunity.

## Materials and Methods

### Mice:

Mice were maintained under specific pathogen-free conditions, and the NCI Animal Care and Use Committee approved all treatments under protocol NCI/LP-012. Breeding pairs of wild type (WT) and B6.129S7-Cd47<sup>tm1Fpl</sup>/J ($Cd47^{-/-}$) C57BL/6J mice (Jackson Laboratory) were back-crossed to minimize genetic drift and obtain $Cd47^{+/-}$ mice. Heterozygous $Cd47^{+/-}$ were bred to obtain $Cd47^{+/+}$, $Cd47^{+/-}$ and $Cd47^{-/-}$ littermate mice. Mouse genotypes were confirmed by PCR using a set of primers targeting the mouse CD47 allele. Littermate and sex-matched mice between 6–12 weeks of age were used for experiments unless otherwise indicated.

Banked cryopreserved B16F10 melanoma cells (obtained from ATCC in 2007) were defrosted and cultured in T-75 flask for 48 hours in complete RPMI 1640 medium containing 5% FBS, 1% PenStrep antibiotics, and 1 mM L-glutamine. Because banked cells at identical passage were used for all animal studies, their identity was not verified in the last year, but the cells were reverified as negative for known murine viruses and mycoplasma by the Animal Health Diagnostic Laboratory, Frederick National Laboratory. WT or $Cd47^{-/-}$ littermate C57BL/6 mice were subcutaneously injected with PBS-washed B16F10 melanoma cells ($1\times10^6$ cells) into the hind limb. Tumor size was measured every other day using calipers for 15 days. In the CD47 blockade studies, doses (intratumoral, 50 μg/mouse) of anti-CD47 miap301 (eBioscience, Cat # 16-0471-85) or isotype rat Ig (eBioscience, Cat # 02–9602) were administered on days 7 and 15, and tumor volume was measured on every other day until day 21.

### Reagents:

DAPI (Cat # D9542), Rat serum (Cat # R9759) and Rabbit serum (Cat # R9133) were purchased from Sigma-Aldrich. Aqua live/dead was from ThermoFisher Scientific (Cat # L3495), UV Zombie was from BioLegend (Cat # 423107), and ACK lysis buffer was purchased from Lonza (Cat # 10–548E).

### NK cell isolation:

Total peripheral NK cell populations from mouse spleens were isolated (> 90% purity) using a NK Isolation Kit II (MACS, Miltenyi Biotec, Cat # 130-115-818) using MACS LS

Columns (Miltenyi Biotec, Cat # 130-042-401) following the manufacturer's instructions. Isolated NK cells were cultured in complete RPMI without or with IL-15 (5–40 ng/ml).

### Cytotoxicity assay:

Purified NK cells from WT and $Cd47^{-/-}$ mouse spleens were tested for their cytotoxic potential against B16 tumor cells. Freshly isolated NK cells or NK cells cultured with IL-15 were incubated with B16 tumor cells with different effector to target ratios (E:T, 1:1, 5:1 and 10:1). Cytotoxicity was determined by measuring the fluorescence intensity of the CellTox Green dye (CellTox™ Green Cytotoxicity, Promega). Fluorescence intensity correlates with the loss of cell membrane integrity caused by cell death. This assay allows real-time kinetic cytotoxicity measurements because the same well can be measured multiple times as the fluorescent signal remains constant after 72 hours. B16 cells (5,000 cells/well) were seeded in 96-well black bottom plates (Greiner). NK cells were added in different E:T ratios to wells containing CellTox Green Dye. Wells without cells were used as a background control. Cell death was determined at 0, 12, 24 and 48 hours of incubation by measuring the fluorescence intensity (485/520 nm excitation/emission) with a TECAN microplate reader. The values obtained from the background control were subtracted from the values obtained from the different experimental conditions.

### Apoptosis analysis:

Cells were stained with annexin V according to the manufacturer instructions (BD Biosciences, Cat # 550474). Cells were washed in PBS and resuspended in $1\times$ annexin binding buffer containing allophycocyanin-conjugated annexin V. After 15 min of incubation at room temperature, cells were diluted in $1\times$ annexin V binding buffer and analyzed by flow cytometry.

### Mitochondrial stress analysis:

Mitochondrial oxygen consumption rate (OCR) and extracellular acidification rate (ECAR) of CD47-sufficient and -deficient NK cells were compared using a Seahorse Bioscience XF$^e$24 analyzer (Massachusetts, USA) in combination with the Seahorse Bioscience XF Cell Mito Stress Test assay kit (Agilent Technologies, Cat # 103015–100). Briefly, NK cells from spleens of WT and $Cd47^{-/-}$ littermate mice were isolated and plated at $0.75\times10^6$ cells/well in 24-well plates (Seahorse Bioscience) into XF Base Medium (Seahorse Bioscience) with added 10 mM glucose, 1 mM sodium pyruvate and 2 mM L-glutamine, pH 7.4. Subsequently, analyses of OCR and EACR were performed in a Seahorse analyzer. The OCR and EACR values were obtained during baseline (prior to addition of any Mito Stress Test substances) and after the addition of 0.5 μM oligomycin, 1 μM FCCP and 0.5 μM rotenone + 0.5 μM antimycin A. Background values from media only were subtracted, and data were corrected by subtracting non-mitochondrial respiration (measured after the injection of rotenone + antimycin A) from all measured OCR values.

### Reactive oxygen species (ROS) assay:

Intracellular ROS of NK cells was quantified using Fluorometric Intracellular ROS Kit (Sigma-Aldrich) according to the manufacturer's instructions. Briefly, isolated NK cells

from WT and littermate *Cd47*^{−/−} mice were subjected to Seahorse Mito stress analysis with ATP synthase inhibitor oligomycin (0.5 μM), mitochondrial uncoupler carbonyl cyanide 4-(trifluoromethoxy) phenylhydrazone (FCCP, 1 μM) and complex I + II inhibitors rotenone (0.5 μM) + antimycin A (0.5 μM). Cells were then incubated with the ROS detection reagent, and the red fluorescence intensity was measured on a flow cytometer.

### RNA extraction, quantitative real-time PCR and Primer sequences:

RNA was purified using the RNeasy Microkit (Qiagen) or TRIzol (Ambion part of Life Technologies) following manufacturer's instructions. RNA content was quantified by NanoDrop 8000 (ThermoFisher Scientific) and 500 ng of RNA was reverse transcribed to cDNA using Thermo Scientific Maxima First Strand cDNA Synthesis Kit (Cat # K1641). Quantitative real-time PCR was performed with SYBR Green using primers for specific genes (Supplementary Table S3) using at least three replicates per group and analyzed on CFX96 Real-time System (BioRad). Relative transcript abundance was determined by using the $C_t$ or $C_t$ method after normalization with *β-Actin* and *Gapdh*. All samples were run in triplicate. Error bars represent S.E.M.

### Tumor processing:

Tumors were cut into small pieces and enzymatically dissociated with Collagenase/Dispase (Roche, Cat # 269638, final concentration 1 mg/ml) and DNase 1 (Sigma, Cat # D4527, final concentration 100 μg/ml). The suspension was centrifuged at 50×g for 5 minutes to separate tissue debris, and supernatant cell suspension was filtered through a 70 μm strainer followed by centrifugation with 330×g for 5 minutes. RBC were lysed using ACK buffer, and cells were suspended in FACS buffer followed by staining or sorting.

### Flow cytometry and cell sorting:

Single cell suspensions from organs and tissues were stained with optimized antibody dilutions for 15 minutes at 4°C (Supplementary Table S4). Antibodies were directly conjugated to Brilliant Ultraviolet (BUV)395, Brilliant Violet (BV)786, BV711, BV650, BV605, Pacific Blue (PB), fluorescein isothiocyanate (FITC), phycoerythrin (PE), PE-Cy5.5, PE-Texas Red, peridinin-chlorophyll-protein complex (PerCP)-Cy5.5, PE-Cy7, allophycocyanin (APC), APC-Alexa 700, or biotin. Biotinylated antibodies were revealed with Streptavidin APCeFluor780. Cells were resuspended in FACS buffer (1% BSA+0.01% NaN$_3$ in PBS1x, filtered) and incubated with rat plus rabbit serum followed by incubation with antibody cocktail against surface molecules. For intracellular staining, cells were fixed (IC Fixation Buffer, eBioscience) and permeabilized (Permeabilization Buffer 10x, eBioscience). Dead cells were excluded through 4,6 diamidino-2-phenylindole (DAPI) uptake or Aqua live/dead staining. Doublets were excluded through forward scatter–height by forward scatter–width and side scatter–height by side scatter–width parameters. Cells were acquired on a LSR Fortessa SORP (BD Biosciences) and data were analyzed using FlowJo (Tree Star). Cell sorting was performed on a FACSAria II (BD Biosciences), and cell purity after sorting was > 99%.

**RNA-seq library construction and Illumina sequencing:**

RNA-seq library preparation and sequencing were performed as in (11). Briefly, Lin$^-$NK1.1$^+$NKp46$^+$ cells were sorted from spleens of naïve and B16F10 tumor-bearing mice. Total RNA was isolated from sorted cells using TRIzol, and DNase treatment was performed using the RNase-free DNase set (Qiagen). RNA quality was checked using an Agilent 2100 Expert bioanalyzer (Agilent Technologies). RNA samples falling below the threshold of 8.0 (scored from 1 to 10) were omitted from the study. Ribosomal RNA was removed using biotinylated, target-specific oligos combined with Ribo-Zero rRNA removal beads. The RNA was fragmented and copied into first strand cDNA, followed by second strand cDNA synthesis using DNA Polymerase I and RNase H. The resulting double-strand cDNA was used as the input to a standard Illumina library prep with end-repair, adapter ligation and PCR amplification being performed. The final purified product was quantitated by qPCR before cluster generation and sequencing. Paired-end sequencing ($2 \times 150$ bp) of stranded total RNA libraries was performed on one HiSeq run with Illumina HiSeq3000/4000 chemistry pair end sequencing. The samples have 99 to 148 million pass filter reads with a base call quality of above 92% of bases with Q30 and above.

HiSeq Real Time Analysis software (RTA 1.18) was used for processing image files. Illumina bcl2fastq1.8.4 was used to demultiplex and convert binary base calls and qualities to fastq format. The sequencing reads were trimmed of adapters and low-quality bases using Trimmomatic (version 0.30), and the trimmed reads were mapped to mouse reference genome (GRCm38/mm10) and Gencode annotation M9 using STAR (version 2.5) with two-pass alignment option. RSEM (version 1.2.22) was used for transcript quantification.

**RNA-seq data processing and analysis:**

The reference genome and annotation from GENECODE Mouse (mm10) was used for further downstream analyses. An in-house pipeline (Pipeliner: https://github.com/CCBR/Pipeliner) was used for data analysis. Briefly, to remove the adapter sequences cutadapt/1.14 was used followed by fastQ Screen v0.9.3 to screen the library for its composition. For quality control the tool fastqc/0.11.5 was used and the spliced transcripts alignment to a reference genome and counting the number of reads per gene was performed by STAR/2.5.2b. The mapped reads in the genomic features were counted by subread/1.5.1 and the distribution of these reads was calculated by rseqc/2.6.4 along with the estimation of strandness of the reads. The library complexity was estimated by preseq/2.0.3. To mark duplicate reads and estimate the gene coverage the program picard/1.119 and for the overall statistics of input datasets samtools/1.5 was used. For differential expression analysis, the low abundant gene threshold was set to include genes with    0.5 counts per million (CPM) in at least    4 samples. In order to generate the gene lists based on different contrast the R Bioconductor package DESeq2 was used. PCA analysis was performed using Partek Genomics Suite (v 6.5) and Gene Set Enrichment Analysis (GSEA) performed using software provided by the Broad Institute. RNAseq data is deposited on the NCBI Sequence Read Archive (GSE113876).

**Statistical analysis:**

Statistical analysis of groups with limited variance was performed using GraphPad Prism 7 (Version 7.01). Comparison between two groups was done via two-sided Student's t-test. Differences with a $p$ value less than 0.05 were considered significant. Error bars indicate standard error of mean (SEM), unless otherwise indicated. cBioPortal tools were used to calculate p-values for TCGA data.

## Results

### CD47 mRNA expression is positively correlated with melanoma overall survival

Consistent with the hypothesis that CD47 protects tumor cells from innate immune surveillance, elevated expression of CD47 in some solid tumors and hematologic malignancies is correlated with a poorer prognosis (24–26). However, analysis of CD47 mRNA expression data in TCGA revealed the opposite for a set of 469 melanomas with RNAseq data, including 461 with survival data (Fig. 1A). Segregating the melanoma RNAseq data with a mean cutoff showed that melanoma patients with tumor CD47 mRNA expression above the mean had significantly longer overall survival than those with expression below the mean (111 months and 62.7 months median survival, respectively, logrank test $p$-value 0.0017). The 65 patients with CD47 expression >1 SD above the mean showed no further improvement (median survival of 103.2 months, logrank test $p$-value 0.14). However, the 85 cases with CD47 mRNA expression more than 1 SD below the mean had a shorter median overall survival of 44.5 months ($p$-value of $6.8 \times 10^{-6}$ compared to the remaining 374 tumors). Disease-free survival was also significantly shorter in the cases with the lowest CD47 expression (36 months versus 56 months, logrank test $p$-value 0.002, Supplementary Fig. S1A). Thus, increased *CD47* gene expression in human melanomas is dose-dependently associated with improved survival.

Because these data were inconsistent with the prevailing "don't eat me" hypothesis, a prediction that tumors with elevated CD47 have poorer survival because they are resistant to phagocytosis by macrophages, we examined co-expressed genes in the TCGA data to identify potential immune mechanisms through which increased intratumoral CD47 mRNA expression could improve melanoma survival. Among the relevant gene sets examined, we identified the highest significance for NK cell-related genes (Fig. 1B). Because significant correlations between expression of these genes and CD47 were generally lacking in other cancers (Supplementary Fig. S1B), this association appears to be specific for melanoma. Using reported gene signatures for naïve versus activated NK cells (27), the highest correlations were observed for an early NK effector signature, and greater than mean expression of one or more of these signature genes was strongly correlated with increased overall survival (148 months versus 48 months (Fig. 1C, $p$-value $6.9 \times 10^{-9}$). Lack of correlation with overall survival in other cancers indicated that the relationship between NK early activation gene expression and outcome is also specific for melanomas (Supplementary Fig. S1C)

A strong positive correlation between CD47 and IL-15 mRNA expression in human melanomas suggested that increased expression of this cytokine could contribute to

activation of NK cells in melanomas that express elevated CD47 (Fig. 1D). Consistent with this hypothesis, IL-15 mRNA expression greater than the mean was associated with improved overall survival ($p$-value $1.5 \times 10^{-8}$) and disease/progression free survival for the melanoma patients ($p$-value $2.3 \times 10^{-3}$, Supplementary Fig. S1D–E).

**Thrombospondin-1 is a CD47-dependent inhibitor for NK cells**

CD47 is an inhibitory receptor for thrombospondin-1 on vascular cells and T cells (28–31). Interaction between CD47 and thrombospondin-1 inhibits TCR signaling in T cells and VEGF-stimulated endothelial cell proliferation (9,30,32). Similarly, a 2 nM concentration of thrombospondin-1, which is sufficient to engage CD47 but not other known thrombospondin-1 receptors, significantly reduced proliferation of isolated murine NK cells as assayed by Ki-67 staining (Fig. 2A). Further, thrombospondin-1 treatment of WT NK cells, but not $Cd47^{-/-}$ NK cells inhibited basal and IL-15 stimulated proliferation as assessed using an MTS assay (Fig. 2B, Supplementary Fig. S2A). Both mRNA and protein expression of CD69 and protein expression of CD11b and CD11c, which are induced upon NK activation (27), were similarly downregulated in LPS-activated NK cells treated with thrombospondin-1 (Fig. 2C–D; Supplementary Fig. S2B,C).

We confirmed the inhibitory activity of thrombospondin-1 using human NK cells. NK-92 cells cultured with IL-2 showed significantly inhibited proliferation in the presence of thrombospondin-1. Such inhibition was reversed when CD47 was blocked using the CD47 antibody B6H12, which similarly stops inhibitory thrombospondin-1 signaling in T cells (33) (Fig.2E). Therefore, the inhibitory activity of thrombospondin-1 requires CD47 in murine and human NK cells.

**Anti-CD47 enhanced intratumor NK cell activity**

The CD47 antibody miap301 similarly blocks inhibitory thrombospondin-1 signaling in murine T cells and enhances syngeneic tumor cell killing by murine CD8 T cells (29,34). Correspondingly, treating murine NK cells with miap301 for 48 hours in culture enhanced cell surface CD69 expression and intracellular IFN$\gamma$. However, intracellular granzyme B (GzmB) was unchanged (Fig. 3A). The response of anti-CD47 treatment was comparable to anti-NK1.1, but not to IL-15 treatment in terms of CD69 expression, GzmB and IFN$\gamma$ (Fig. 3A). Lack of these responses in $Cd47^{-/-}$ NK cells confirmed specificity (Fig. 3B).

Extending the *in vitro* enhancement of NK cell function by miap301 to study NK cell immunity in a mouse tumor model is complicated by the dual function of this antibody to block both thrombospondin-1 and SIRP$\alpha$ binding. The anti-human CD47 B6H12 is efficacious in multiple xenograft tumor models, which is attributed to enhancing SIRP$\alpha$-dependent phagocytic clearance by macrophages, but miap301 generally does not inhibit growth of syngeneic tumors in immune competent mice (25). Therefore, we tested the effect of miap301 on NK cell function in the syngeneic B16 model. Intratumoral anti-CD47 treatment with miap301 slowed the growth of B16 tumors compared to tumors in mice treated with isotype-matched rat Ig (Fig. 3C). Treatment of tumor-infiltrating NK cells isolated from B16 tumors treated with miap301 but not the control antibody significantly increased intracellular IFN$\gamma$ after 48 hours of treatment (Fig. 3D–F). Such *in vitro* treatment

increased intracellular IFN$\gamma$ and GzmB levels in B16 infiltrating NK cells but not in infiltrating CD8 T cells (Fig. 3G–I). Therefore, our previously reported increase in intratumoral granzyme B expression following CD47 knockdown in several syngenic tumor models may be produced primarily by NK cells (6).

## Expression of CD47 on NK cells limits their proliferation and effector state

IL-15 dose-dependently increased the frequency of NK1.1$^+$ cells in cultured WT and *Cd47*$^{-/-}$ splenocytes, but the response to IL-15 was greater in *Cd47*$^{-/-}$ (Fig. 4A). Similarly, cell activation and proliferation, assessed by CD69 and Ki-67 staining respectively, was enhanced in *Cd47*$^{-/-}$ NK1.1$^+$ cells (Fig. 4B). Intracellular GzmB staining of splenic NK cells from naïve *Cd47*$^{-/-}$ mice trended to be higher in frequency and count but did not achieve significance (Supplementary Fig. S3A). The MFI of IFN$\gamma$ and GzmB were comparable between WT and *Cd47*$^{-/-}$ total splenocytes and NK1.1$^+$ populations within the total splenocytes cultured with increasing dosages of IL-15 (Supplementary Fig. S3B–C). NK cells isolated from the spleens of WT and *Cd47*$^{-/-}$ mice cultured with IL-15 for 24 hours exhibited down-regulated CD44 and up-regulated CD62L surface expression (Fig. 4C; Supplementary Fig. S3D). However, *Cd47*$^{-/-}$ NK cells were more CD44 positive and less CD62L positive compared to the WT NK cells (Fig. 4C). An increasing trend of GzmB, T-bet, KLRG1 and TNF-$\alpha$ was evident in IL-15 treated *Cd47*$^{-/-}$ NK cells relative to similarly treated WT NK cells (Fig. 4D, Supplementary Fig. S3E). IL-15 treatment significantly upregulated EOMES and T-bet expression in *Cd47*$^{-/-}$ NK cells relative to that in WT NK cells (Fig. 4E). However, *in vitro* cytotoxic activities of WT and *Cd47*$^{-/-}$ NK cells, both with and without IL-15 treatment, were comparable when co-cultured with target B16 melanoma cells (Supplementary Fig. S3F).

After continuous culture with IL-15 for 72 hours, a decreasing trend of IFN$\gamma$ and GzmB protein labels was evident in *Cd47*$^{-/-}$ total splenocytes relative to WT counterparts (Supplementary Fig. S4A). Analysis of similarly cultured *Cd47*$^{+/-}$ NK cells revealed that the decrease of *Ifng* and *Gzmb* transcripts was CD47 dose-dependent (Supplementary Fig. S4B).

Global transcriptome analysis of WT and *Cd47*$^{-/-}$ NK cells from spleens of naïve mice identified 2585 genes to be significantly upregulated ($p < 0.05$) in naïve *Cd47*$^{-/-}$ versus WT NK cells, including the effector genes *Ifna2* (IFN$\alpha$2), *Ifna4* (IFN$\alpha$4), *Ifna13* (IFN$\alpha$13), *Gzmc* (granzyme C), *Il2ra* (CD25), *Mapk13* (MAPK13) and *Jun* (c-Jun) (Supplementary Fig. S5A; Supplementary Table 1). As expected, *Cd47* was significantly decreased in *Cd47*$^{-/-}$ NK cells (Supplementary Fig. S5A, Supplementary Table S1). An unsupervised Gene set enrichment analysis (GSEA) showed upregulation of early effector, sustained effector, interferon and proliferation gene signatures, whereas naïve and memory gene signatures were downregulated in naïve *Cd47*$^{-/-}$ NK cells compared to WT counterparts (Supplementary Fig. S5B, Supplementary Table S2).

Pathway analysis showed altered responses of NK cells in the absence of *Cd47*. An upregulation of immune-related pathways including immune response (G:0002376, GO:0002682, GO:0050776, R-HAS-168249, GO:0006955), cytokine production and signal transduction (go:0007165) (Supplementary Fig. S3C) as well as significant downregulation

of NK-mediated cytotoxicity, MAPK, EGFR and DAP12 signaling pathways were evident in $Cd47^{-/-}$ NK cells (Supplementary Fig. S5C). Cytoscape functional and molecular interaction networks in NK cells revealed that the immune and inflammation related genes were significantly altered upon $Cd47$ depletion (Supplementary fig. S5D).

**CD47 limits mitochondrial metabolism and ROS production in NK cells**

CD47 controls mitochondrial homeostasis and metabolism and, in T cells, apoptosis pathways involving the mitochondrial regulators Drp1 and BNIP3 (32,35–37). Mitochondrial electron transport can generate reactive oxygen species (ROS) that control intrinsic apoptosis pathways (38). Global gene expression analysis demonstrated that the top upregulated pathways in $Cd47^{-/-}$ NK cells include metabolic regulation and ion transport, whereas, the top downregulated pathways include mitochondrial protein regulation and mitochondrial organization (Supplementary Fig. S5C). To investigate whether CD47 regulates mitochondrial and glycolytic metabolism in NK-cells, we measured the mitochondrial oxygen consumption rate (OCR) and extracellular acidification rate (ECAR) in NK cells subjected to mitochondrial stress. Sequentially blocking key enzymes of the respiratory chain of mitochondria using oligomycin, FCCP, and a mix of rotenone and antimycin A was performed to measure ATP production, maximum respiration, and nonmitochondrial respiration, respectively. Basal mitochondrial flux assessed by OCR values was similar for WT and $Cd47^{-/-}$ NK cells. In contrast, basal glycolytic flux assessed by ECAR values was higher in $Cd47^{-/-}$ NK cells (Fig. 5A–B). The ATP turnover values in WT and $Cd47^{-/-}$ NK cells were comparable (56.6±19.4 verses 67.2±0.3). However, the proton leak values in $Cd47^{-/-}$ NK cells (38.7±13.5) were higher than in WT NK cells (14.5±0.5). In addition, the spare respiratory capacity in $Cd47^{-/-}$ NK cells (191.9±20.7) was higher than in WT NK cells (151.1±9.2). Therefore, WT and $Cd47^{-/-}$ NK cells differ in glucose metabolism and respond differently to inhibition or uncoupling of mitochondrial respiratory pathways.

We measured the ROS in WT and $Cd47^{-/-}$ NK cells after 1 and 24 hours of cell culture with oligomycin, FCCP, rotenone, and antimycin A. The frequency of intracellular ROS-positive $Cd47^{-/-}$ NK cells was higher than in WT NK cells subjected to one hour of mitochondrial stress (Fig. 5C). Incubation for 24 hours with the mitochondrial stressors upregulated intracellular ROS accumulation both in WT and $Cd47^{-/-}$ NK cells, with a significantly higher mean intracellular ROS intensity in $Cd47^{-/-}$ NK cells than in WT NK cells (Fig. 5C).

**CD47-deficient NK cells undergo apoptosis upon stimulation or under stress**

The higher metabolic activity and mitochondrial stress responses of CD47-deficient NK cells results in accumulation of more intracellular ROS, suggesting that CD47-deficiency may increase NK cell apoptosis. Annexin V staining of untreated NK cells from WT and $Cd47^{-/-}$ mice was comparable. However, mitochondrial stress induced by treating NK cells with oligomycin, FCCP, rotenone plus antimycin A for 24 hours resulted in higher annexin V-positive staining of $Cd47^{-/-}$ NK cells (Fig. 5D–F).

## CD47-deficiency in the tumor microenvironment augments B16 melanoma growth

We previously reported that combining antisense CD47 morpholino knockdown and local tumor irradiation or local irradiation of B16 tumors in $Cd47^{-/-}$ mice significantly delays the growth of B16 melanoma relative to irradiation alone in immune-competent C57BL/6 mice (6,39). However, CD47 knockdown in the absence of irradiation only minimally affected B16 tumor growth (6,39). Implanted B16 tumors grew faster in $Cd47^{-/-}$ than in WT mice (Fig. 6A–C).

B16 tumor cells elicit a weak cytotoxic T cell response due to downregulated MHC class I expression (40), suggesting that the reported CD8 T cell-dependent tumor ablation could also involve NK cells. Frequencies of NK1.1$^+$ and NKp46$^+$ NK cells significantly dropped within the spleens of $Cd47^{-/-}$ mice on day 15 post B16 melanoma implantation (Fig. 6D–G). Flow cytometric analysis of the NK1.1$^+$ compartment in spleens showed a significant increase of CD44 and decrease of CD62L levels in $Cd47^{-/-}$ NK cells compared to WT counterparts (Fig. 6H–I). Reduction of CD62L level in $Cd47^{-/-}$ NK cells following *in vitro* stimulation (Fig. 4C) as well as in tumor-bearing mice indicates reduced functionality of $Cd47^{-/-}$ NK cells. Concomitantly, increased expression of the exhaustion marker TIGIT and the ATPase CD39 within the CD62L$^+$ population of CD47-deficient NK cells further indicated an exhausted and apoptotic phenotype (Fig. 6J–K). Eomesodermin (Eomes) is the master transcriptional regulator of NK cell development, maturation and function (41) and is downregulated in exhausted NK cells in leukemic mice (42). Similarly, splenic NK cells from $Cd47^{-/-}$ tumor-bearing mice exhibited a decreasing trend of Eomes (Fig. 6L). CD127 expression on NK cells correlates with lower granzyme B level and a defect in activation (43), and the CD127 level was significantly increased in CD47-deficient NK cells of tumor bearing mice (Fig. 6M). KLGR1 expression differentiates effector and memory NK cells (44). However, KLRG1 expression did not differ between B16-bearing WT and $Cd47^{-/-}$ mice at day 15 (Fig. 6N). Tumor-experienced NK cells express significantly higher level of PD-1 and PD-L1, suggesting NK exhaustion as well as inhibitory immune regulation (45,46). Upregulation of PD-1 was also associated with decreased degranulation and impaired cytokine production (45,47). Consistent with these studies, $Cd47^{-/-}$ NK cells expressed significantly higher levels of PD-1 and PD-L1 and significantly less intracellular granzyme B compared to WT NK cells (Fig. 6O–Q).

## CD47 in the tumor microenvironment controls transcriptional reprogramming of NK cells

We performed global transcriptome analysis of intratumoral and splenic NK cells at day 15 post implantation of B16 melanoma in WT and $Cd47^{-/-}$ mice. Intratumoral NK cells from WT and $Cd47^{-/-}$ mice showed a low RNA integrity value (Supplementary Fig. S6A) and high divergence by principal component analysis, which precluded further analysis. Therefore, we focused on systemic changes in splenic NK cells. Delineation of population relationships with the three most informative principal components showed segregation of the population into four discrete clusters (Fig. 7A). Comprehensive pairwise comparison of NK cells showed up-regulation of around 3000 genes in WT tumor-bearing compared to WT naïve mice. However, many fewer genes were upregulated in $Cd47^{-/-}$ NK cells (total number= 705) than in WT NK cells (total number= 3012) from tumor-bearing mice (Fig. 7B, Supplementary Table 1). Differential upregulation of inhibitory genes including *Cish*

(CIS), *Mmp9* (MMP-9), *Lag3* (CD223), *Havcr2* (Tim-3), *Tigit* (TIGIT) and *Pdcd1* (PD-1) and downregulation of activation genes including *Sell* (CD62L), *Mcam* (CD146), *Klrk1* (NKG2D) and *Klrc2* (NKG2C) were evident in NK cells from tumor-bearing $Cd47^{-/-}$ mice relative to WT counterparts (Fig. 7C, Supplementary Fig. S6B–D).

As observed in NK cells from naïve mice (11), significant negative enrichments of naïve and memory NK cell signatures were evident in $Cd47^{-/-}$ NK cells from tumor-bearing mice, but sustained effector and proliferation gene signatures were positively enriched in $Cd47^{-/-}$ NK cells from tumor-bearing mice (Fig. 7D, Supplementary Table 2). Consistent with our earlier observation (Fig. 5D–F), a proapoptotic gene signature (Qiagen GeneGlobe: Apoptosis and Cell Death, species = mouse) was also upregulated in splenic NK cells from tumor-bearing $Cd47^{-/-}$ mice (Fig. 7D). Similarly, pathway analysis revealed upregulation of gene ontologies involved in negative regulation of cell cycle phase transition (GO:0045786, GO:0010948), apoptosis (R-HSA-109581, GO:0042981), programmed cell death (R-HSA-5357801), and intrinsic apoptotic signaling (GO:0008630) and downregulation of signal transduction (GO:0009966), TCR signaling (cd8tcrpathway), response to endogenous stimulus (GO:0009719), mTOR signaling (hsa04150) and response to hypoxia (GO:0001666) pathways in $Cd47^{-/-}$ NK cell from tumor-bearing mice (Supplementary Fig. S7). These data suggest a globally impaired NK cell immune response in B16 melanoma-bearing $Cd47^{-/-}$ mice.

## Discussion

Cytotoxic NK cells are key effectors in cancer immune surveillance, transplantation rejection, and viral immunity (48). TCGA data identified positive correlations for CD47 expression with patient survival and enrichment of NK cell activation markers. Among the cancers analyzed, these correlations are unique to melanomas. Using mouse models and antibody blockade we identified positive and negative roles for CD47 in regulating NK cell recruitment, activation, proliferation and survival in the tumor microenvironment. CD47 in NK cells is a cell-intrinsic inhibitory signaling receptor for thrombospondin-1 that limits NK proliferation and activation, consistent with the known CD47-dependent inhibitory functions of thrombospondin-1 in T cells and vascular cells (8,30). Thrombospondin-1 inhibits TCR-induced proliferation and CD69 induction in a CD47-dependent manner in T cells (8,30) and inhibited LPS-induced Ki-67 and CD69 expression in NK cells. Treatment with a CD47 blocking antibody reversed thrombospondin-1 inhibition in a human NK cell line, inhibited tumor growth in mice bearing B16 melanoma, and increased tumoral NK cell recruitment and expression of granzyme B and interferon-γ.

Conversely, we observed a CD47-dependent increase of exhaustion markers in splenic NK cells of melanoma tumor bearing mice. Immune cell exhaustion has been associated with chronic infection and cancer (49,50), and sustained infection and tumor growth may lead to NK cell exhaustion (48,51–55). Downregulation of NK activating receptors including NKG2D, CD16, CD146 and NCRs and/or upregulation of certain NK inhibitory receptors like PD-1, LAG3, TIM-3 or TIGIT are hallmarks of NK cell exhaustion (56). Activating receptor NKG2D is frequently downregulated on NK cells in cancer patients as well as chronic virus infected patients (27,57). Similarly, inhibitory receptor Tim-3 was upregulated

in cancer and chronic hepatitis B patients and significantly decreased cytotoxicity of peripheral NK cells (58,59). The cytokine-inducible SH2-containing protein (CIS) has been identified as a critical negative regulator in NK-mediated tumor immunity (60). CIS is a key suppressor of IL-15 signaling promoting NK cell death and limiting proliferation, IFN$\gamma$ production and cytotoxicity towards B16 melanoma (60). Similarly, *Mmp9* mediates NK cell dysfunction and augments tumor resistance to NK cytotoxicity within the tumor microenvironment (61,62). Phenotypic changes and altered expression of these genes consistent with NK exhaustion and dysfunction were found in CD47-deficient NK cells isolated from the spleen of B16 bearing mice, indicating that CD47 systemically protects NK cells from exhaustion. However, our data does not exclude additional contributions of previously reported altered angiogenic and adaptive immune functions in *Cd47*-deficient mice to the faster growth of B16 tumors.

CD47 regulates NK cell transcriptional responses to activating stimuli, and its absence results in a defect in mitochondrial metabolism. CD47 is a known regulator of mitochondrial homeostasis and metabolism (32,37). Consistent with those studies, $Cd47^{-/-}$ NK cells exhibit an increased spare respiratory capacity. The increased mitochondrial proton leak in NK cells and increased intracellular reactive oxygen species (ROS) production in $Cd47^{-/-}$ NK cells subjected to mitochondrial stress is consistent with the observed apoptotic phenotype. Induction of apoptosis in cytotoxic NK cells after activation is an essential mechanism to prevent autoimmunity (63–65). Mitochondria release pro-apoptotic factors including ROS and cytochrome-c that activate apoptosis programs in cytolytic lymphocytes, CD8 T cells and NK cells, during the contraction phase (66–68). A resulting systemic depletion of NK cells in $Cd47^{-/-}$ mice may contribute to the augmented chronic LCMV infection (11) and B16 melanoma growth. Thus, CD47 has a cell-intrinsic protective function in NK cells that sustains their survival under chronic stress conditions.

Integrins regulated by CD47 play positive roles in T cell migration and in immune synapse formation (69). Further studies are required to delineate whether defective integrin activation contributes to the impaired NK responses to B16 melanoma in $Cd47^{-/-}$ mice. Integrin signaling also limits apoptosis, which could contribute to the apoptotic signature of $Cd47^{-/-}$ NK cells in challenged mice (70). Although the absence of CD47 enhances mature NK cell numbers in naïve mice (11), the increased apoptotic signature in challenged mice could result in surface markers that, in the absence of a CD47 don't eat me signal, could lead to increased phagocytic clearance of $Cd47^{-/-}$ NK cells.

Gene set enrichment suggests that CD47 mediates distinct effects on gene expression in naïve, effector, and memory NK cells. Furthermore, because all immune cell types express CD47, we do not expect that NK cells exclusively mediate the observed functions of CD47 in the tumor microenvironment that regulate melanoma growth.

Our findings have implications for the ongoing clinical development of humanized CD47 antibodies and other biologics that target CD47. Most of the preclinical tumor models supporting these trials were performed using xenogeneic NOD/SCID mice that lack T and B cells but have NK cells and macrophages. Unlike macrophages, NK cells do not express SIRP$\alpha$ but express more CD47 than other lymphocytes (11). If these experimental

therapeutics also disrupt the thrombospondin-1-CD47 interaction, they might promote the antitumor activity of NK cells. CD47 antibody treatment could thereby promote activation of systemic and tumor-associated NK cells. The resulting enhanced production of granzyme B and IFNγ by tumor infiltrating NK cells could contribute to the antitumor efficacy of experimental CD47 therapeutics by increasing direct NK cytotoxicity in addition to the known effects on tumor-associated macrophages.

In summary, these results identify important roles of CD47 in NK cell immune responses to human and murine melanomas. Some of the observed regulation of NK cell activities involves CD47 functioning as an inhibitory signaling receptor for thrombospondin-1, but additional CD47 signaling in NK cells may be mediated by its lateral interactions with integrins and other signaling receptors. Given the essential role of NK cells in tumor immunity, additional studies are needed to define how experimental therapeutics impact CD47-SIRPα versus thrombospondin-1-CD47 signaling in NK cells and to assess their direct effects on antitumor activities of NK cells. Understanding how CD47 signaling in NK cells impacts tumor cell killing when combined with cytotoxic or targeted agents may lead to more effective application of these therapeutics.

## Supplementary Material

Refer to Web version on PubMed Central for supplementary material.

## Acknowledgements:

## References:

1. Barclay AN, Van den Berg TK. The interaction between signal regulatory protein alpha (SIRPalpha) and CD47: structure, function, and therapeutic target. Annu Rev Immunol 2014;32:25–50 doi 10.1146/annurev-immunol-032713-120142. [PubMed: 24215318]

2. Oldenborg P, Zheleznyak A, Fang Y, Lagenaur CF, Gresham HD, Lindberg FP. Role of CD47 as a marker of self on red blood cells. Science 2000;288(5473):2051–4 doi 10.1126/science. 288.5473.2051. [PubMed: 10856220]

3. Soto-Pantoja DR, Kaur S, Roberts DD. CD47 signaling pathways controlling cellular differentiation and responses to stress. Critical reviews in biochemistry and molecular biology 2015;50(3):212–30 doi 10.3109/10409238.2015.1014024. [PubMed: 25708195]

4. Matlung HL, Szilagyi K, Barclay NA, van den Berg TK. The CD47-SIRPalpha signaling axis as an innate immune checkpoint in cancer. Immunological reviews 2017;276(1):145–64 doi 10.1111/imr. 12527. [PubMed: 28258703]

5. Kwong LS, Brown MH, Barclay AN, Hatherley D. Signal-regulatory protein alpha from the NOD mouse binds human CD47 with an exceptionally high affinity-- implications for engraftment of human cells. Immunology 2014;143(1):61–7 doi 10.1111/imm.12290. [PubMed: 24786312]

6. Soto-Pantoja DR, Terabe M, Ghosh A, Ridnour LA, DeGraff WG, Wink DA, et al. CD47 in the tumor microenvironment limits cooperation between antitumor T-cell immunity and radiotherapy. Cancer Res 2014;74(23):6771–83 doi 10.1158/0008-5472.CAN-14-0037-T. [PubMed: 25297630]

7. Sockolosky JT, Dougan M, Ingram JR, Ho CC, Kauke MJ, Almo SC, et al. Durable antitumor responses to CD47 blockade require adaptive immune stimulation. Proc Natl Acad Sci U S A 2016;113(19):E2646–54 doi 10.1073/pnas.1604268113. [PubMed: 27091975]

8. Miller TW, Kaur S, Ivins-O'Keefe K, Roberts DD. Thrombospondin-1 is a CD47-dependent endogenous inhibitor of hydrogen sulfide signaling in T cell activation. Matrix biology : journal of the International Society for Matrix Biology 2013;32(6):316–24 doi 10.1016/j.matbio.2013.02.009. [PubMed: 23499828]

9. Kaur S, Kuznetsova SA, Pendrak ML, Sipes JM, Romeo MJ, Li Z, et al. Heparan sulfate modification of the transmembrane receptor CD47 is necessary for inhibition of T cell receptor signaling by thrombospondin-1. The Journal of biological chemistry 2011;286(17):14991–5002 doi 10.1074/jbc.M110.179663. [PubMed: 21343308]

10. Weng TY, Huang SS, Yen MC, Lin CC, Chen YL, Lin CM, et al. A novel cancer therapeutic using thrombospondin 1 in dendritic cells. Mol Ther 2014;22(2):292–302 doi 10.1038/mt.2013.236. [PubMed: 24127010]

11. Nath PR, Gangaplara A, Pal-Nath D, Mandal A, Maric D, Sipes JM, et al. CD47 Expression in Natural Killer Cells Regulates Homeostasis and Modulates Immune Response to Lymphocytic Choriomeningitis Virus. Front Immunol 2018;9:2985 doi 10.3389/fimmu.2018.02985. [PubMed: 30643501]

12. Spits H, Bernink JH, Lanier L. NK cells and type 1 innate lymphoid cells: partners in host defense. Nat Immunol 2016;17(7):758–64 doi 10.1038/ni.3482. [PubMed: 27328005]

13. Arnon TI, Achdout H, Lieberman N, Gazit R, Gonen-Gross T, Katz G, et al. The mechanisms controlling the recognition of tumor- and virus-infected cells by NKp46. Blood 2004;103(2):664–72. doi 10.1182/blood-2003-05-1716 [PubMed: 14504081]

14. Halfteck GG, Elboim M, Gur C, Achdout H, Ghadially H, Mandelboim O. Enhanced in vivo growth of lymphoma tumors in the absence of the NK-activating receptor NKp46/NCR1. J Immunol 2009;182(4):2221–30 doi 10.4049/jimmunol.0801878 [PubMed: 19201876]

15. Pegram HJ, Andrews DM, Smyth MJ, Darcy PK, Kershaw MH. Activating and inhibitory receptors of natural killer cells. Immunol Cell Biol 2011;89(2):216–24 doi 10.1038/icb.2010.78. [PubMed: 20567250]

16. Trowsdale J. Genetic and Functional Relationships between MHC and NK Receptor Genes. Immunity 2001;15(3):363–74 doi 10.1016/S1074-7613(01)00197-2. [PubMed: 11567627]

17. Orr MT, Lanier LL. Natural killer cell education and tolerance. Cell 2010;142(6):847–56 doi 10.1016/j.cell.2010.08.031. [PubMed: 20850008]

18. Anfossi N, Andre P, Guia S, Falk CS, Roetynck S, Stewart CA, et al. Human NK cell education by inhibitory receptors for MHC class I. Immunity 2006;25(2):331–42 doi 10.1016/j.immuni.2006.06.013. [PubMed: 16901727]

19. Saunders PM, Vivian JP, O'Connor GM, Sullivan LC, Pymm P, Rossjohn J. A bird's eye view of NK cell receptor interactions with their MHC class I ligands. Immunological reviews 2015;267(1):148–66 doi 10.1111/imr.12319. [PubMed: 26284476]

20. Pierson BA, Gupta K, Hu WS, Miller JS. Human natural killer cell expansion is regulated by thrombospondin-mediated activation of transforming growth factor-beta 1 and independent accessory cell-derived contact and soluble factors. Blood 1996;87(1):180–9. [PubMed: 8547640]

21. Legrand N, Huntington ND, Nagasawa M, Bakker AQ, Schotte R, Strick-Marchand H, et al. Functional CD47/signal regulatory protein alpha (SIRP(alpha)) interaction is required for optimal human T- and natural killer- (NK) cell homeostasis in vivo. Proc Natl Acad Sci U S A 2011;108(32):13224–9 doi 10.1073/pnas.1101398108. [PubMed: 21788504]

22. Kim MJ, Lee JC, Lee JJ, Kim S, Lee SG, Park SW, et al. Association of CD47 with natural killer cell-mediated cytotoxicity of head-and-neck squamous cell carcinoma lines. Tumour Biol 2008;29(1):28–34 doi 10.1159/000132568. [PubMed: 18497546]

23. Yanagita T, Murata Y, Tanaka D, Motegi SI, Arai E, Daniwijaya EW, et al. Anti-SIRPalpha antibodies as a potential new tool for cancer immunotherapy. JCI Insight 2017;2(1):e89140 doi 10.1172/jci.insight.89140. [PubMed: 28097229]

24. Chao MP, Weissman IL, Majeti R. The CD47-SIRPalpha pathway in cancer immune evasion and potential therapeutic implications. Curr Opin Immunol 2012;24(2):225–32 doi 10.1016/j.coi. 2012.01.010. [PubMed: 22310103]

25. Willingham SB, Volkmer JP, Gentles AJ, Sahoo D, Dalerba P, Mitra SS, et al. The CD47-signal regulatory protein alpha (SIRPa) interaction is a therapeutic target for human solid tumors. Proc Natl Acad Sci U S A 2012;109(17):6662–7 doi 10.1073/pnas.1121623109. [PubMed: 22451913]

26. Majeti R, Chao MP, Alizadeh AA, Pang WW, Jaiswal S, Gibbs KD Jr., et al. CD47 is an adverse prognostic factor and therapeutic antibody target on human acute myeloid leukemia stem cells. Cell 2009;138(2):286–99 doi 10.1016/j.cell.2009.05.045. [PubMed: 19632179]

27. Bezman NA, Kim CC, Sun JC, Min-Oo G, Hendricks DW, Kamimura Y, et al. Molecular definition of the identity and activation of natural killer cells. Nat Immunol 2012;13(10):1000–9 doi 10.1038/ni.2395. [PubMed: 22902830]

28. Gao Q, Chen K, Gao L, Zheng Y, Yang YG. Thrombospondin-1 signaling through CD47 inhibits cell cycle progression and induces senescence in endothelial cells. Cell death & disease 2016;7(9):e2368 doi 10.1038/cddis.2016.155. [PubMed: 27607583]

29. Kaur S, Chang T, Singh SP, Lim L, Mannan P, Garfield SH, et al. CD47 signaling regulates the immunosuppressive activity of VEGF in T cells. J Immunol 2014;193(8):3914–24 doi 10.4049/jimmunol.1303116. [PubMed: 25200950]

30. Kaur S, Martin-Manso G, Pendrak ML, Garfield SH, Isenberg JS, Roberts DD. Thrombospondin-1 inhibits VEGF receptor-2 signaling by disrupting its association with CD47. The Journal of biological chemistry 2010;285(50):38923–32 doi 10.1074/jbc.M110.172304. [PubMed: 20923780]

31. Kaur S, Soto-Pantoja DR, Stein EV, Liu C, Elkahloun AG, Pendrak ML, et al. Thrombospondin-1 signaling through CD47 inhibits self-renewal by regulating c-Myc and other stem cell transcription factors. Sci Rep 2013;3:1673 doi 10.1038/srep01673. [PubMed: 23591719]

32. Miller TW, Soto-Pantoja DR, Schwartz AL, Sipes JM, DeGraff WG, Ridnour LA, et al. CD47 Receptor Globally Regulates Metabolic Pathways That Control Resistance to Ionizing Radiation. The Journal of biological chemistry 2015;290(41):24858–74 doi 10.1074/jbc.M115.665752. [PubMed: 26311851]

33. Li Z, He L, Wilson KE, Roberts DD. Thrombospondin-1 Inhibits TCR-Mediated T Lymphocyte Early Activation. The Journal of Immunology 2001;166(4):2427–36 doi 10.4049/jimmunol. 166.4.2427. [PubMed: 11160302]

34. Soto-Pantoja DR, Shih HB, Maxhimer JB, Cook KL, Ghosh A, Isenberg JS, et al. Thrombospondin-1 and CD47 signaling regulate healing of thermal injury in mice. Matrix biology : journal of the International Society for Matrix Biology 2014;37:25–34 doi 10.1016/j.matbio.2014.05.003. [PubMed: 24840925]

35. Lamy L, Ticchioni M, Rouquette-Jazdanian AK, Samson M, Deckert M, Greenberg AH, et al. CD47 and the 19 kDa interacting protein-3 (BNIP3) in T cell apoptosis. The Journal of biological chemistry 2003;278(26):23915–21 doi 10.1074/jbc.M301869200. [PubMed: 12690108]

36. Bras M, Yuste VJ, Roue G, Barbier S, Sancho P, Virely C, et al. Drp1 mediates caspase-independent type III cell death in normal and leukemic cells. Molecular and cellular biology 2007;27(20):7073–88 doi 10.1128/mcb.02116-06. [PubMed: 17682056]

37. Frazier EP, Isenberg JS, Shiva S, Zhao L, Schlesinger P, Dimitry J, et al. Age-dependent regulation of skeletal muscle mitochondria by the thrombospondin-1 receptor CD47. Matrix biology : journal of the International Society for Matrix Biology 2011;30(2):154–61 doi 10.1016/j.matbio. 2010.12.004. [PubMed: 21256215]

38. Green DR, Galluzzi L, Kroemer G. Cell biology. Metabolic control of cell death. Science 2014;345(6203):1250256 doi 10.1126/science.1250256. [PubMed: 25237106]

39. Maxhimer JB, Soto-Pantoja DR, Ridnour LA, Shih HB, Degraff WG, Tsokos M, et al. Radioprotection in normal tissue and delayed tumor growth by blockade of CD47 signaling. Science translational medicine 2009;1(3):3ra7 doi 10.1126/scitranslmed.3000139.

40. Seliger B, Wollscheid U, Momburg F, Blankenstein T, Huber C. Characterization of the major histocompatibility complex class I deficiencies in B16 melanoma cells. Cancer Res 2001;61(3): 1095–9. [PubMed: 11221838]

41. Simonetta F, Pradier A, Roosnek E. T-bet and Eomesodermin in NK Cell Development, Maturation, and Function. Front Immunol 2016;7:241 doi 10.3389/fimmu.2016.00241. [PubMed: 27379101]

42. Gill S, Vasey AE, De Souza A, Baker J, Smith AT, Kohrt HE, et al. Rapid development of exhaustion and down-regulation of eomesodermin limit the antitumor activity of adoptively transferred murine natural killer cells. Blood 2012;119(24):5758–68 doi 10.1182/blood-2012-03-415364. [PubMed: 22544698]

43. Gasteiger G, Hemmers S, Bos PD, Sun JC, Rudensky AY. IL-2-dependent adaptive control of NK cell homeostasis. The Journal of experimental medicine 2013;210(6):1179–87 doi 10.1084/jem.20122571. [PubMed: 23650439]

44. Kamimura Y, Lanier LL. Homeostatic control of memory cell progenitors in the natural killer cell lineage. Cell Rep 2015;10(2):280–91 doi 10.1016/j.celrep.2014.12.025. [PubMed: 25578733]

45. Beldi-Ferchiou A, Lambert M, Dogniaux S, Vély F, Vivier E, Olive D, et al. PD-1 mediates functional exhaustion of activated NK cells in patients with Kaposi sarcoma. Oncotarget 2016;7(45):72961–77 doi: 10.18632/oncotarget.12150. [PubMed: 27662664]

46. Fuertes MB, Iraolagoitia XLR, Ziblat A, Nuñez SY, Torres NI, Secchiari F, et al. Tumor-experienced human NK cells express PD-L1 and display immunoregulatory functions. J Immunol 2017;198(1):Supplement 56.2.

47. Pesce S, Greppi M, Tabellini G, Rampinelli F, Parolini S, Olive D, et al. Identification of a subset of human natural killer cells expressing high levels of programmed death 1: A phenotypic and functional characterization. J Allergy Clin Immunol 2017;139(1):335–46 e3 doi 10.1016/j.jaci.2016.04.025. [PubMed: 27372564]

48. Vivier E, Tomasello E, Baratin M, Walzer T, Ugolini S. Functions of natural killer cells. Nat Immunol 2008;9(5):503–10 doi 10.1038/ni1582. [PubMed: 18425107]

49. Wherry EJ. T cell exhaustion. Nature Immunology 2011;131(6):492–9 doi 10.1038/ni.2035.

50. Joyce JA, Fearon DT. T cell exclusion, immune privilege, and the tumor microenvironment. Science 2015;348(6230):74–80 doi 10.1126/science.aaa6204. [PubMed: 25838376]

51. Herberman RB, Nunn ME, Holden HT, Larvin DH. Natural cytotoxic reactivity of mouse lymphoid cells against syngeneic and allogeneic tumors. II. Characterization of effector cells. Int J Cancer 1975;16(2):230–9 doi 10.1002/ijc.2910160205. [PubMed: 1080480]

52. Kiessling R, Klein E, Wigzell H. "Natural" killer cells in the mouse. I. Cytotoxic cells with specificity for mouse Moloney leukemia cells. Specificity and distribution according to genotype. Eur J Immunol 1975;5(2):112–7 doi 10.1002/eji.1830050208. [PubMed: 1234049]

53. Vivier E, Ugolini S, Blaise D, Chabannon C, Brossay L. Targeting natural killer cells and natural killer T cells in cancer. Nat Rev Immunol 2012;12:239–52. [PubMed: 22437937]

54. Alvarez-Breckenridge CA, Yu J, Price R, Wojton J, Pradarelli J, Mao H, et al. NK cells impede glioblastoma virotherapy through NKp30 and NKp46 natural cytotoxicity receptors. Nat Med 2012;18(12):1827–34 doi 10.1038/nm.3013. [PubMed: 23178246]

55. Guillerey C, Ferrari de Andrade L, Vuckovic S, Miles K, Ngiow SF, Yong MC, et al. Immunosurveillance and therapy of multiple myeloma are CD226 dependent. J Clin Invest 2015;125(5):2077–89 doi 10.1172/JCI77181. [PubMed: 25893601]

56. Kared H, Martelli S, Tan SW, Simoni Y, Chong ML, Yap SH, et al. Adaptive NKG2C+CD57+ Natural Killer Cell and Tim-3 Expression During Viral Infections. Frontiers in Immunology 2018;9:686 doi 10.3389/fimmu.2018.00686 [PubMed: 29731749]

57. Mamessier E, Sylvain A, Thibult ML, Houvenaeghel G, Jacquemier J, Castellano R, et al. Human breast cancer cells enhance self tolerance by promoting evasion from NK cell antitumor immunity. J Clin Invest 2011;121(9):3609–22 doi 10.1172/JCI45816. [PubMed: 21841316]

58. Sun C, Xu J, Huang Q, Huang M, Wen H, Zhang C, et al. High NKG2A expression contributes to NK cell exhaustion and predicts a poor prognosis of patients with liver cancer. Oncoimmunology 2017;6(1):e1264562 doi 10.1080/2162402X.2016.1264562. [PubMed: 28197391]

59. Baba N, Van VQ, Wakahara K, Rubio M, Fortin G, Panzini B, et al. CD47 fusion protein targets CD172a+ cells in Crohn's disease and dampens the production of IL-1beta and TNF. The Journal of experimental medicine 2013;210(6):1251–63 doi 10.1084/jem.20122037. [PubMed: 23669395]

60. Delconte RB, Kolesnik TB, Dagley LF, Rautela J, Shi W, Putz EM, et al. CIS is a potent checkpoint in NK cell-mediated tumor immunity. Nat Immunol 2016;17(7):816–24 doi 10.1038/ni.3470. [PubMed: 27213690]

61. Albertsson PA, Basse PH, Hokland M, Goldfarb RH, Nagelkerke JF, Nannmark U, et al. NK cells and the tumour microenvironment: implications for NK-cell function and anti-tumour activity. Trends in immunology 2003;24(11):603–9. [PubMed: 14596885]

62. Fiore E, Fusco C, Romero P, Stamenkovic I. Matrix metalloproteinase 9 (MMP-9/gelatinase B) proteolytically cleaves ICAM-1 and participates in tumor cell resistance to natural killer cell-mediated cytotoxicity. Oncogene 2002;21(34):5213–23 doi 10.1038/sj.onc.1205684. [PubMed: 12149643]

63. Daniels KA, Devora G, Lai WC, O'Donnell CL, Bennett M, Welsh RM. Murine cytomegalovirus is regulated by a discrete subset of natural killer cells reactive with monoclonal antibody to Ly49H. The Journal of experimental medicine 2001;194(1):29–44 doi 10.1084/jem.194.1.29. [PubMed: 11435470]

64. Dokun AO, Kim S, Smith HR, Kang HS, Chu DT, Yokoyama WM. Specific and nonspecific NK cell activation during virus infection. Nat Immunol 2001;2(10):951–6 doi 10.1038/ni714. [PubMed: 11550009]

65. Sun JC, Beilke JN, Lanier LL. Adaptive immune features of natural killer cells. Nature 2009;457(7229):557–61 doi 10.1038/nature07665. [PubMed: 19136945]

66. Min-Oo G, Bezman NA, Madera S, Sun JC, Lanier LL. Proapoptotic Bim regulates antigen-specific NK cell contraction and the generation of the memory NK cell pool after cytomegalovirus infection. The Journal of experimental medicine 2014;211(7):1289–96 doi 10.1084/jem.20132459. [PubMed: 24958849]

67. Kroemer G, Reed JC. Mitochondrial control of cell death. Nat Med 2000;6(5):513–9. [PubMed: 10802706]

68. Grayson JM, Laniewski NG, Lanier JG, Ahmed R. Mitochondrial Potential and Reactive Oxygen Intermediates in Antigen-Specific CD8+ T Cells During Viral Infection. The Journal of Immunology 2003;170(9):4745–51 doi 10.4049/jimmunol.170.9.4745. [PubMed: 12707355]

69. Azcutia V, Routledge M, Williams MR, Newton G, Frazier WA, Manica A, et al. CD47 plays a critical role in T-cell recruitment by regulation of LFA-1 and VLA-4 integrin adhesive functions. Mol Biol Cell 2013;24(21):3358–68 doi 10.1091/mbc.E13-01-0063. [PubMed: 24006483]

70. Streuli CH. Integrins and cell-fate determination. J Cell Sci 2009;122(Pt 2):171–7 doi 10.1242/jcs.018945. [PubMed: 19118209]

## Synopsis

Identification of NK-cell immune checkpoints in the tumor microenvironment could provide a basis for improving melanoma treatment. CD47 expression regulated intratumoral and systemic NK-cell function, with blockade of CD47 improving antitumor NK-cell responses in melanoma.
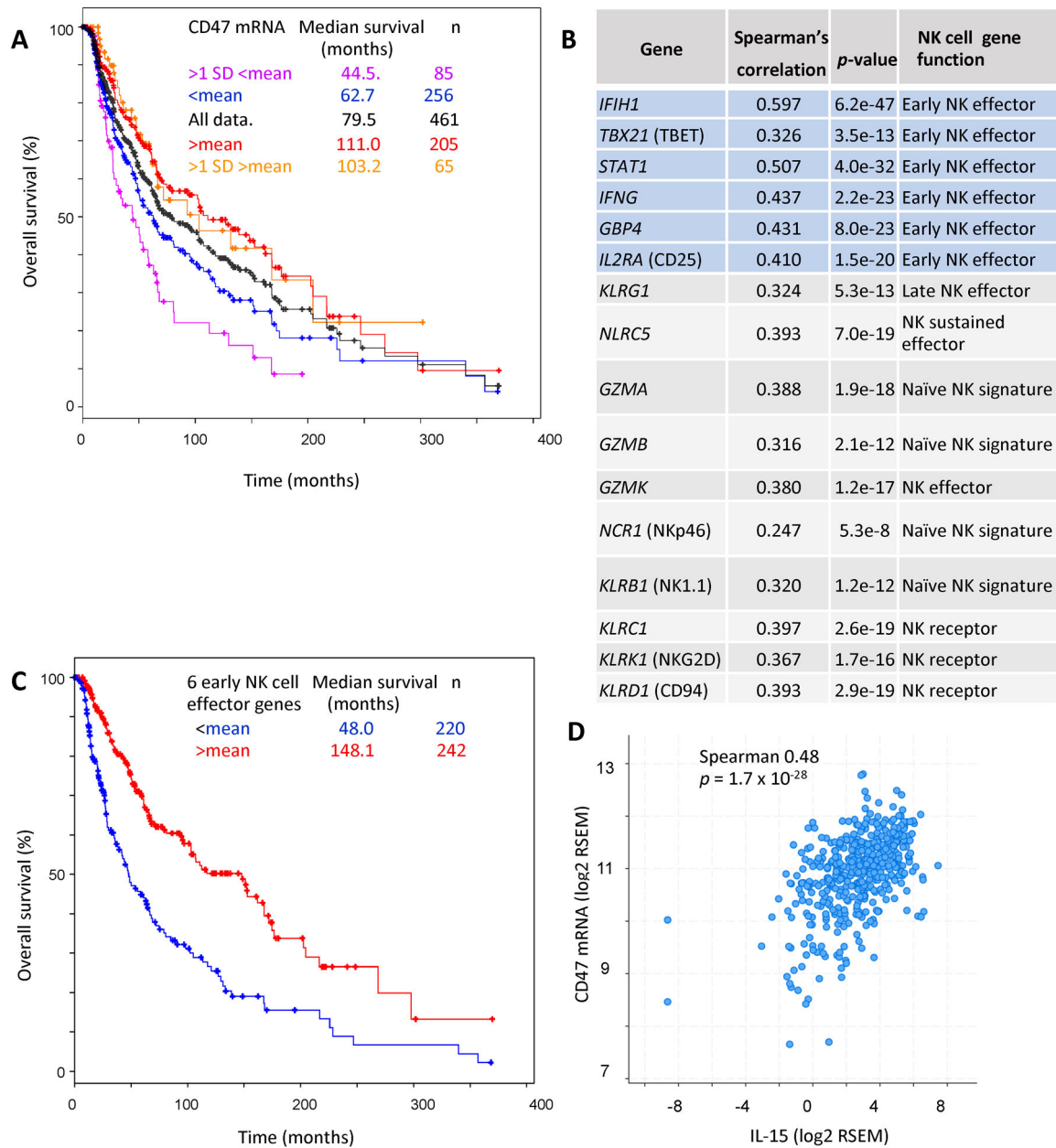
**A**



| CD47 mRNA | Median survival (months) | n |
|---|---|---|
| >1 SD <mean | 44.5. | 85 |
| <mean | 62.7 | 256 |
| All data. | 79.5 | 461 |
| >mean | 111.0 | 205 |
| >1 SD >mean | 103.2 | 65 |

**B**

| Gene | Spearman's correlation | p-value | NK cell gene function |
|---|---|---|---|
| *IFIH1* | 0.597 | 6.2e-47 | Early NK effector |
| *TBX21* (TBET) | 0.326 | 3.5e-13 | Early NK effector |
| *STAT1* | 0.507 | 4.0e-32 | Early NK effector |
| *IFNG* | 0.437 | 2.2e-23 | Early NK effector |
| *GBP4* | 0.431 | 8.0e-23 | Early NK effector |
| *IL2RA* (CD25) | 0.410 | 1.5e-20 | Early NK effector |
| *KLRG1* | 0.324 | 5.3e-13 | Late NK effector |
| *NLRC5* | 0.393 | 7.0e-19 | NK sustained effector |
| *GZMA* | 0.388 | 1.9e-18 | Naïve NK signature |
| *GZMB* | 0.316 | 2.1e-12 | Naïve NK signature |
| *GZMK* | 0.380 | 1.2e-17 | NK effector |
| *NCR1* (NKp46) | 0.247 | 5.3e-8 | Naïve NK signature |
| *KLRB1* (NK1.1) | 0.320 | 1.2e-12 | Naïve NK signature |
| *KLRC1* | 0.397 | 2.6e-19 | NK receptor |
| *KLRK1* (NKG2D) | 0.367 | 1.7e-16 | NK receptor |
| *KLRD1* (CD94) | 0.393 | 2.9e-19 | NK receptor |

**C**



| 6 early NK cell effector genes | Median survival (months) | n |
|---|---|---|
| <mean | 48.0 | 220 |
| >mean | 148.1 | 242 |

**D**



Spearman 0.48
$p = 1.7 \times 10^{-28}$

**Figure 1. Improved survival of melanoma patients with elevated CD47 expression is associated with markers of early effector NK cells.**
(**A**) Dose-dependent correlation between CD47 mRNA expression and overall survival in TCGA melanoma data. (**B**) Analysis of TCGA RNAseq data for co-expression correlations between CD47 mRNA and naïve or activated NK signature genes as defined in (27). Spearman's correlation and *p*-values determined using cBioPortal tools are presented for TCGA RNAseq data from 469 cutaneous melanoma patients. (**C**) Overall survival of patients with mRNA expression of the 6 early NK effector signature genes greater than (red) or less than the mean (blue) aggregate values determined by RNAseq analysis (n = 462 patients). (**D**) IL-15 expression correlates with IL-15 mRNA expression in TCGA melanoma data. (n = 469 patients)

Author Manuscript
Author Manuscript
Author Manuscript
Author Manuscript

**A**



**B**



**C**

CD69



**D**



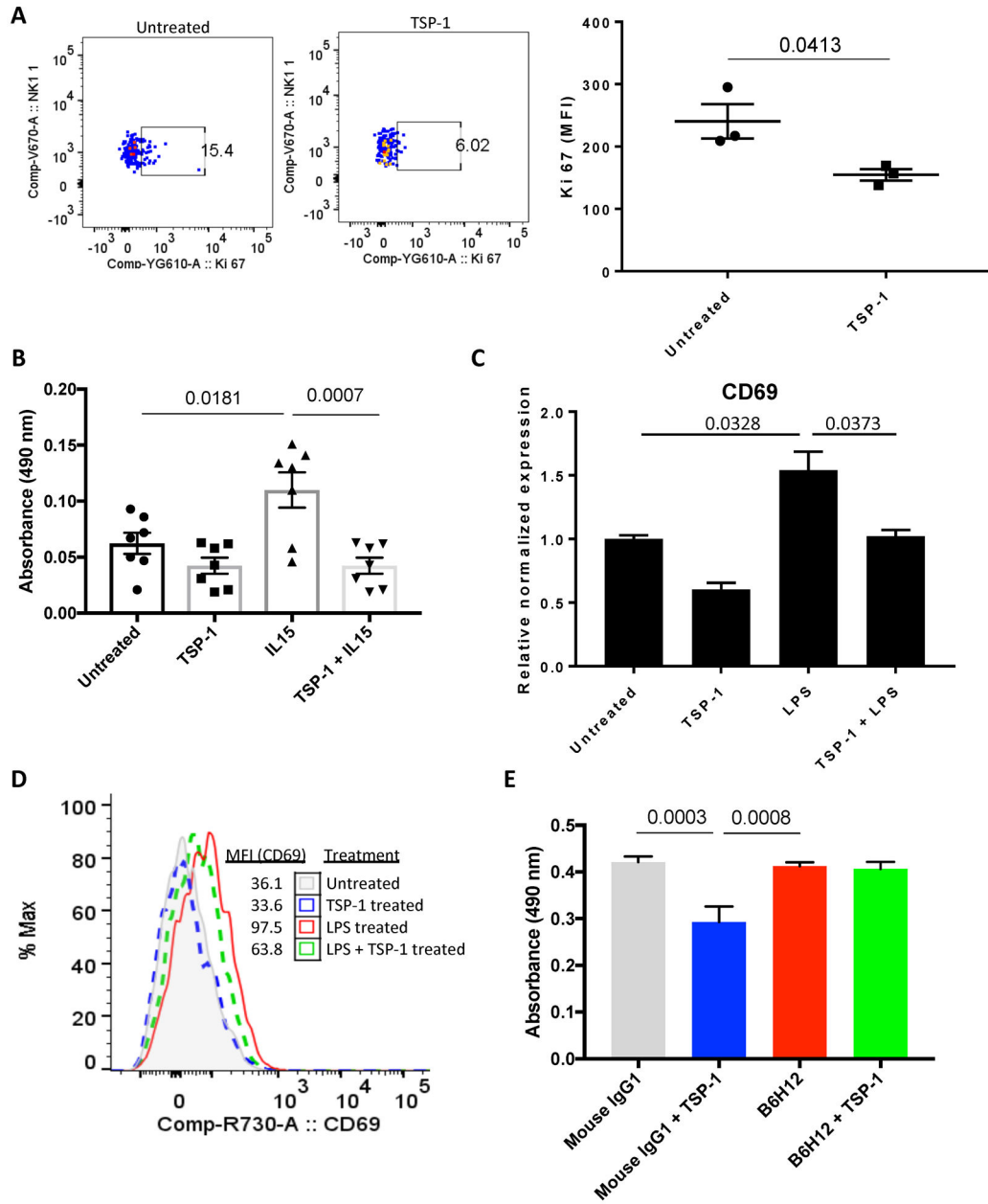| MFI (CD69) | Treatment |
|---|---|
| 36.1 | Untreated |
| 33.6 | TSP-1 treated |
| 97.5 | LPS treated |
| 63.8 | LPS + TSP-1 treated |

**E**



**Figure 2: Thrombospondin-1 inhibits NK cell proliferation and activation**

NK cells were isolated from spleens of WT mice by MACS NK isolation kit. **(A)** Cells were cultured in serum free RPMI for 24 hours with/out thrombospondin-1 (2 nM) followed by fixation, permeabilization and i.c. staining for Ki-67, n = 3 biological replicates, error bars indicate standard error of the mean (SEM). **(B)** NK cells were cultured in serum free RPMI with/without IL-15 (10 ng/ml) and MTS absorbance was measured after 24 hrs of culture in the presence or absence of thrombospondin-1 (2 nM), n = 7 biological replicates, error bars indicate SEM. **(C)** Isolated NK cells were divided into 4 groups and cultured in serum free RPMI with thrombospondin-1 (2 nM), LPS (1 µg/ml) or both. mRNA abundance (relative to *β-Actin*) and **(D)** cell surface protein levels of CD69 were measured by RT-qPCR (LPS

versus TSP-1+LPS treatments, $P = 0.0373$, n = 3 biological replicates, error bars indicate SEM) and flow cytometry (representative), respectively. **(E)** Human NK-92 cells were cultured in serum free RPMI with 100 IU IL-2 and treated either with mouse IgG (1 ug/ml) or B6H12 (1 ug/ml) in the presence or absence of human thrombospondin-1 (2 nM) and MTS absorbance was measured after 48 hrs, n = 5 technical replicates, error bars indicate SEM.
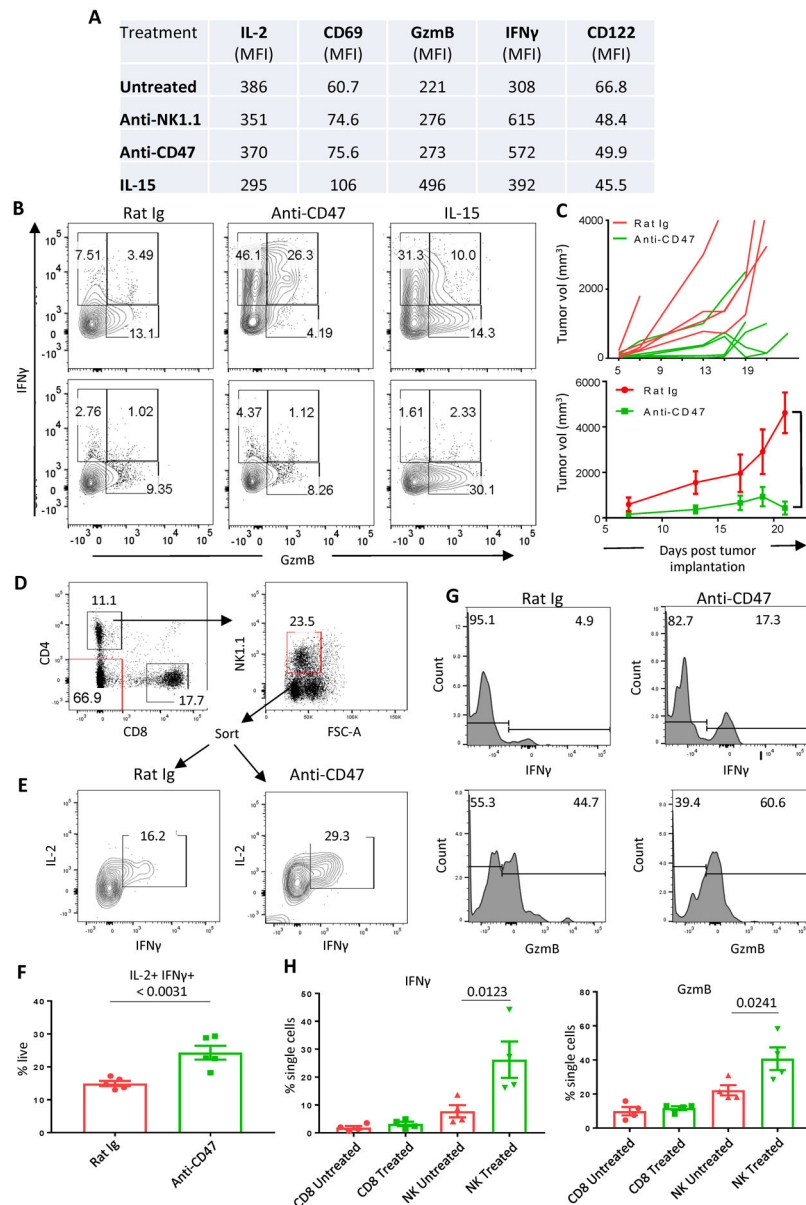
**Figure 3. Miap301-treatment enhances effector protein expression in NK cells and reduces tumor growth**

**(A)** NK cells were isolated from WT spleens and treated with anti-CD47 (miap301, 5 ug/ ml), anti-NK1.1 (5 ug/ml) or IL-15 (40 ng/ml) for 48 hrs with Golgi-stop at last 4 hrs in culture, n = 3 biological replicates. Table shows the MFI of IL2, CD69, GzmB, IFNγ and CD122 proteins within different treatment groups. **(B)** Plots show intracellular expression of GzmB and IFNγ in isotype rat Ig, anti-CD47 and IL-15 treated WT and *Cd47*^{−/−} NK cells. **(C)** B16F10 tumors were implanted in the hindlimb of C57BL/6 mice and two doses of rat Ig or anti-CD47 Ab (intra-tumoral, 50 μg/mouse) were administered on day 7 and 15. Tumor volume was measured on every other day. WT versus *Cd47*^{−/−} mice, *P* = 0.001, n= 5 biological replicates, error bars indicate SEM. **(D-E)** Animals were sacrificed on day 21, tumors were incised, DAPI^{−}CD45.2^{+}CD4^{−}CD8^{−}CD3^{−}NK1.1^{+} cells were sorted from single

cell suspension and treated with rat Ig (5 ug/ml) or anti-CD47 (5 ug/ml) for 48 hrs with Golgi-stop during the last 4 hours in culture. Cells were intracellular stained for IL-2 and IFNγ, n=5. **(F-I)** Representative plots and frequencies of intracellular IFNγ and GzmB expression in rat Ig or anti-CD47 treated tumor infiltrating CD8 T and NK cells, n= 4–5 biological replicates, error bars indicate SEM.
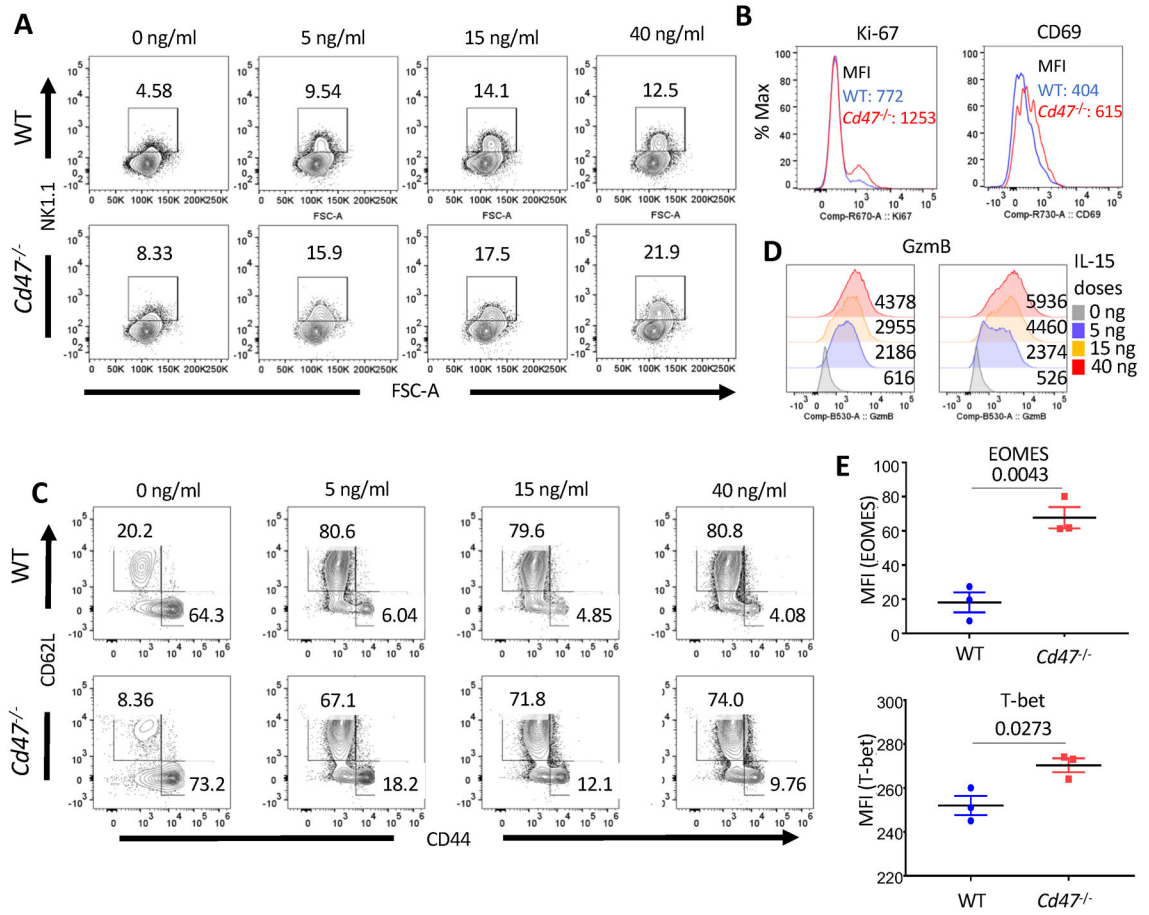
**Figure 4. CD47 limits some effector properties of NK cell**

(**A**) Single cell suspensions from a pool of 3 WT and 3 *Cd47*$^{-/-}$ littermate mice spleens were treated with IL-15 (5, 15 and 40 ng/ml) for 24 hrs in complete RPMI (10% FCS). Cells were FcR-blocked and stained for Aqua live/dead, NK1.1 and CD69, followed by i.c. staining for Ki-67. Frequencies of NK1.1+ cells within the cultured splenocytes were detected by flowcytometry. Data is representative of two independent experiments. (**B**) Histograms show expression of Ki-67 and CD69 within the NK1.1$^+$ population of IL-15 (5 ng/ml) treated group. Values on the plots are MFI of indicated protein in NK1.1$^+$ cells. Data is representative of two independent experiments. (**C**) NK cells were enriched from pooled splenocytes of WT and *Cd47*$^{-/-}$ littermate mice and cultured with IL-15 (5, 15 and 40 ng/ml) for 24 hrs and stained for CD44 and CD62L. Data is representative of two independent experiments. (**D**) Histograms show expression of granzyme B (GzmB) within the NK1.1$^+$ population, values indicate MFI in NK1.1$^+$ cells. Data is representative of two independent experiments. (**E**) NK cells from the spleens of WT and *Cd47*$^{-/-}$ littermate mice were treated with IL-15 (5 ng/ml for 24 hrs) and stained for intracellular EOMES (*P* = 0.0043) and T-bet (*P* = 0.0273) proteins, n = 3 biological replicates, error bars indicate SEM.
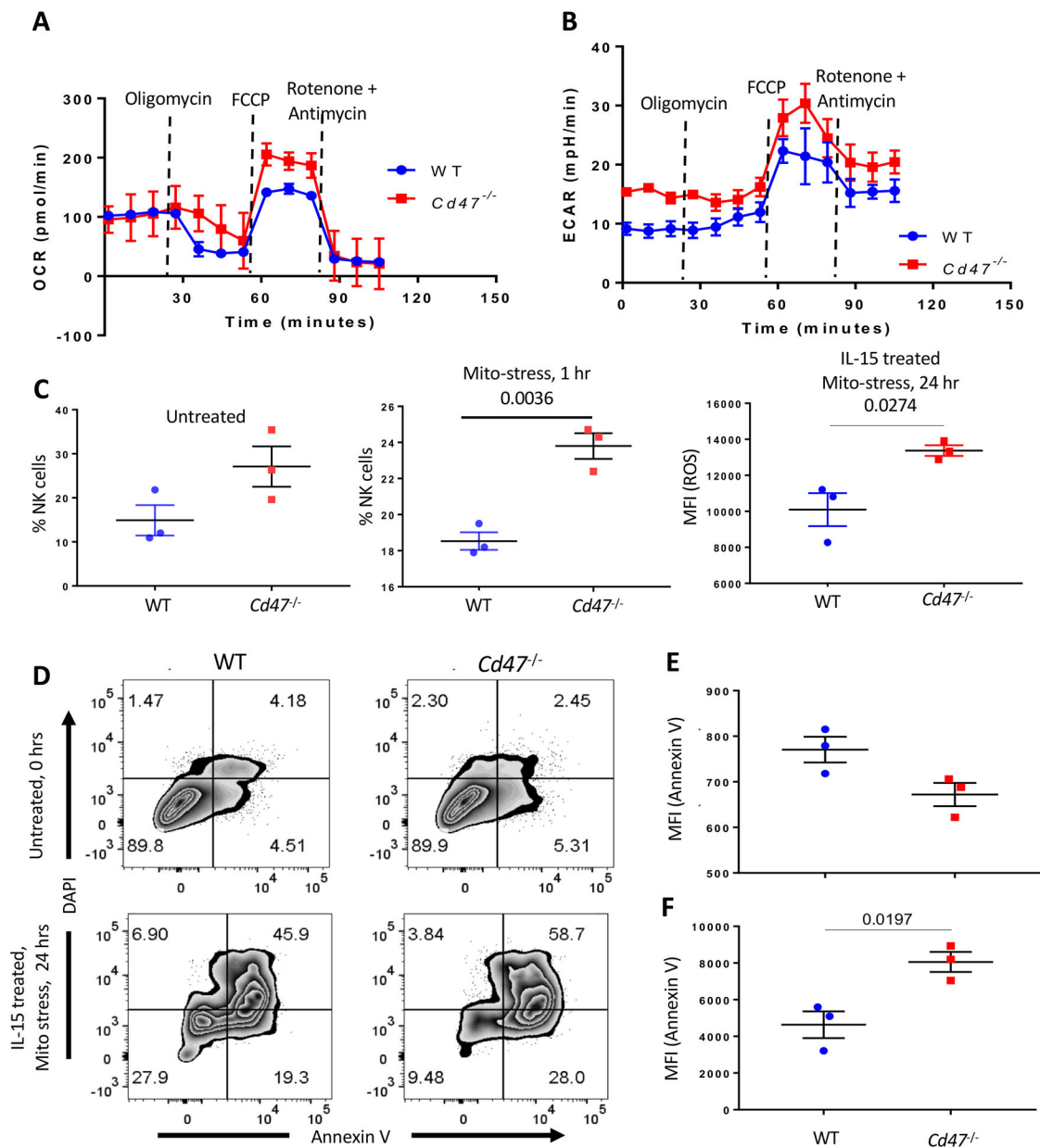
**Figure 5. CD47 limits mitochrondrial metabolism, intracellular ROS accumulation and apoptosis of NK cells**

NK cells were isolated from pooled spleens of WT and *Cd47*^{−/−} mice and subjected to mitochondrial-stress by sequential injecting oligomycin, FCCP and a mix of rotenone and antimycin A, n = pool of 3 biological replicates, error bars indicate SEM. **(A)** OCR and **(B)** ECAR measured at different time points. **(C)** Intracellular ROS accumulation was measured in WT and *Cd47*^{−/−} untreated, 1 hour and 24 hours mito-stress treated NK cells, n = 3 biological replicates, error bars indicate SEM. **(D)** Annexin V staining of WT and *Cd47*^{−/−} NK cells, untreated or treated with mitochondrial-stress. **(E-F)** MFI of annexin V staining in untreated and mitochondrial-stress treated NK cells from spleens of WT and *Cd47*^{−/−} mice, n = 3 biological replicates, error bars indicate SEM.
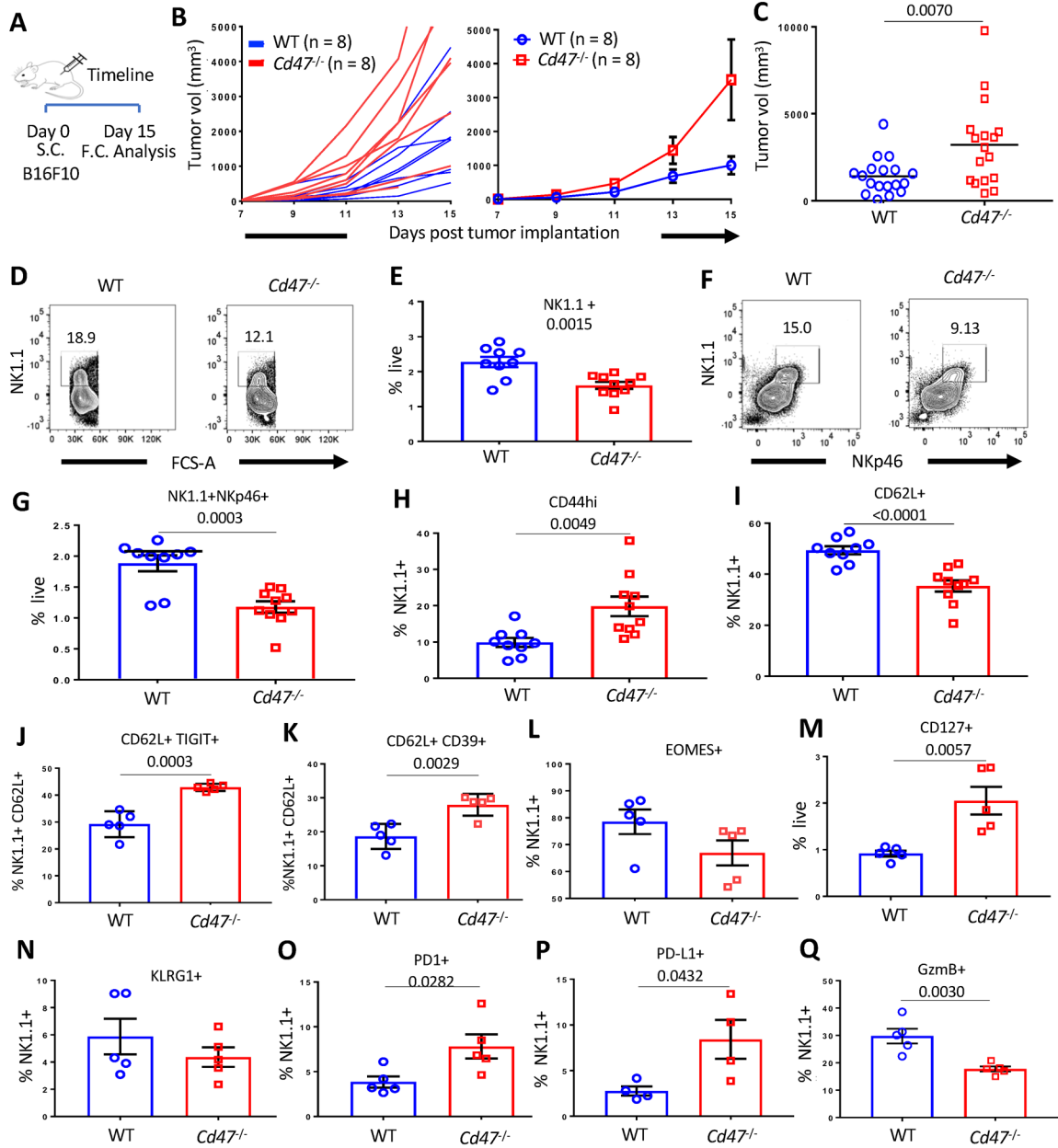
**Figure 6. CD47 limits the growth of B16F10 melanoma in mice**

(**A**) Timeline of B16F10 tumor implantation and analysis of mice. B16F10 tumors were implanted in the hind-limb of C57BL/6 WT and $Cd47^{-/-}$ littermate mice ($1 \times 10^6$ cells/ mouse). On day 15 post tumor implantation, mice were euthanized, and single cell suspensions of spleens were stained with Lin-cocktail (anti-CD4, -CD8, -TCRβ, -B220, -CD19, -Gr1 and -Ter119), anti-NK1.1 and anti-NKp46 in FACS buffer containing Aqua live/ dead. Cells were then fixed, permeabilized and intracellular stained for the indicated proteins. (**B**) Tumor volume was measured on every other day for two weeks. n = 8 biological replicates, error bars indicate SEM. (**C**) Tumor volume was measured on day 15 post tumor implantation (WT versus $Cd47^{-/-}$ mice, $P = 0.007$, n = 17–18 mice per group).

**(D-G)** Representative plots and frequency of live Lin⁻NK1.1⁺ cells (WT versus $Cd47^{-/-}$ mice, $P = 0.0015$) and Lin⁻NK1.1⁺NKp46⁺ cells (WT versus $Cd47^{-/-}$ mice, $P = 0.0003$) at day 15 post tumor implantation are shown within the spleens of the mice. n = 9–10 mice per group. **(H-I, L-Q)** Frequency of CD44 (WT versus $Cd47^{-/-}$ mice, $P = 0.0049$), CD62L (WT versus $Cd47^{-/-}$ mice, $p < 0.0001$), Eomes, CD127 (WT versus $Cd47^{-/-}$ mice, $P = 0.0057$), KLRG1, PD-1 (WT versus $Cd47^{-/-}$ mice, $P = 0.0282$), PD-L1 (WT versus $Cd47^{-/-}$ mice, $P = 0.0432$), and granzyme B (GzmB, WT versus $Cd47^{-/-}$ mice, $P = 0.003$) positive NK cells within the spleens of tumor bearing mice. n = 4–5 mice per group, error bars indicate SEM. **(J-K)** Frequency of TIGIT (WT versus $Cd47^{-/-}$ mice, $P = 0.0003$) and CD39 (WT versus $Cd47^{-/-}$ mice, $P = 0.0029$) positive population within CD62L positive compartment of NK cells. n = 4–5 mice per group, error bars indicate SEM. All data are representative of two independent experiments.
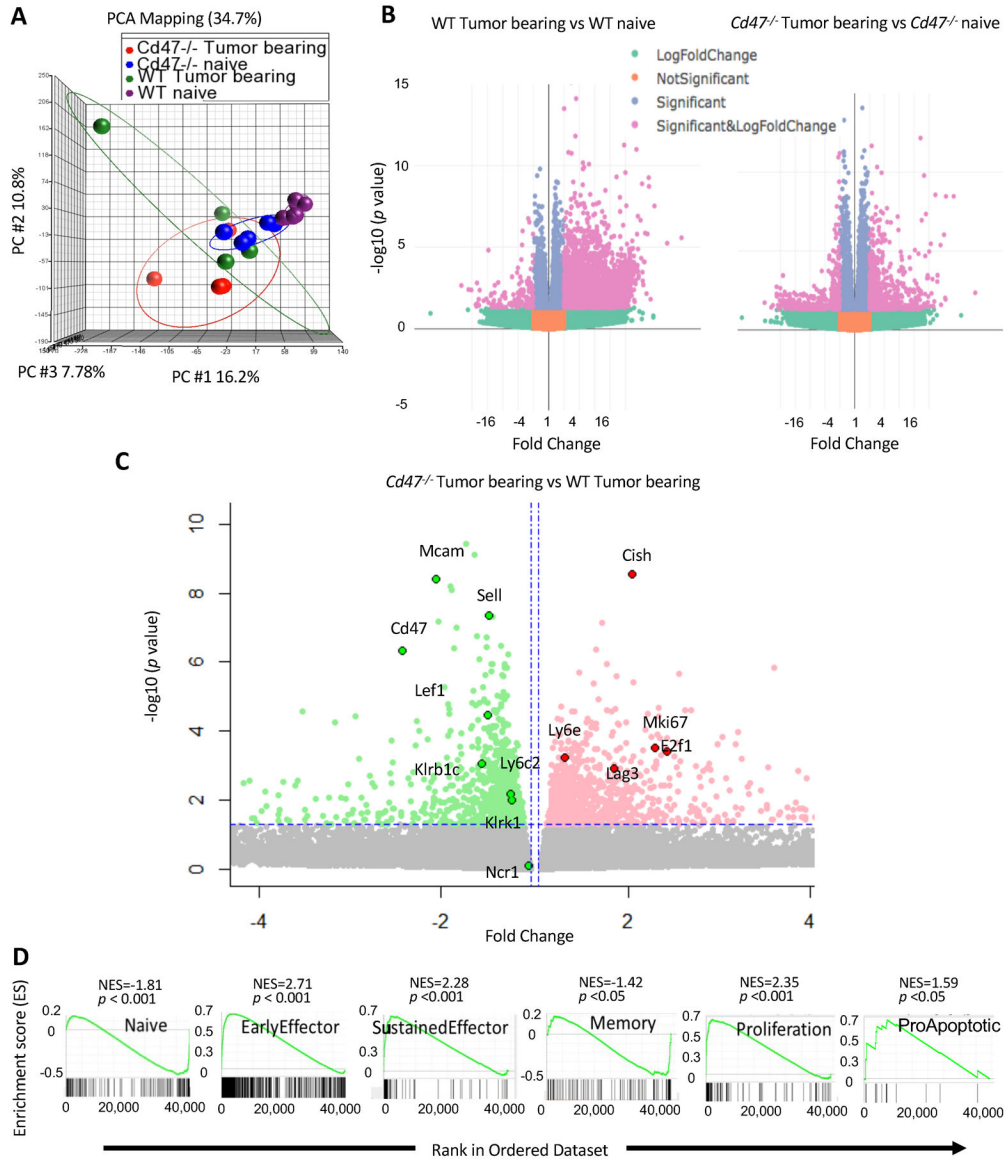
**Figure 7. Transcriptional profile of splenic CD47-deficient NK cells varies from CD47-sufficient NK cells in a murine melanoma model**

**(A)** Principle component analysis (PCA) on global transcriptome data shows four distinct clusters of naïve WT, naïve $Cd47^{-/-}$, B16-tumor bearing WT and B16-tumor bearing $Cd47^{-/-}$ NK cells. **(B)** Volcano plots show that number of genes upregulated in NK cells of B16 bearing mice compared to their naïve counterparts. **(C)** Volcano plot displaying fold change of genes in NK cells of $Cd47^{-/-}$ mice than in WT mice bearing B16 tumor. **(D)** GSEA plots in $Cd47^{-/-}$ compared to WT NK cell of B16 bearing mice.